Newton-Raphson Power-Flow Analysis Including Induction Motor Loads

Pichai Aree[1], Non-member

ABSTRACT

This paper presents an extended method of Newton-Raphson power flow algorithm to incorporate nonlinear model of induction motor loads. The proposed method is used for finding correct power system operating conditions, which can be employed for solving the problem of initializing the dynamic models of induction motor for stability studies. The power flow solution with a group of induction motor loads is demonstrated through 14buses industrial power system. Moreover, the computational efficiency of the extended algorithm has been investigated using IEEE-30buses network. The results show that this algorithm gives an exact solution of motor's active and reactive powers that are related with converged slips, terminal voltages, and mechanical torque profiles. Furthermore, the extended algorithm shows a good convergent characteristic in quadratic manner.

Keywords: Power Flow Analysis, Induction Motor Load

1. INTRODUCTION

The problem of power system voltage and transient stabilities due to dynamic behavior of induction motor loads has been a major area of attractions for planner and operation engineers all over the world [1-2]. The research studies show that the induction motor loads play an important role on the power system stabilities when the systems are heavily stressed. For dynamic studies and stability assessment, initializing the power system with the motor loads using the converged power flow solution is required as starting point [3-4]. Generally, the current industry practice is to obtain power flow solution with induction motors represented by normal PQ load (constant power type). The initial active and reactive powers of induction motors are scheduled. After the power flow solution successfully converges, the initial active power and the converged voltage are employed to compute the actual values of motor's reactive power. At this point, the differences between the actual and the scheduled reactive powers are compensated by a fictitious admittance that is added into the load bus admittance matrix [4-5]. For example, if the actual reactive power of the motor is greater than the reactive power initially scheduled, the value of compensating capacitor is automatically calculated. Then, this capacitor will be placed at the motor terminal bus. This initializing method may not provide the exact value of the motor reactive power consumption and may not yield a meaningful analysis in dynamic studies and stability assessments [6-7].

The IEEE Task Force on Load Representation of Dynamic Performance [4] pointed out the need for further development of accurate procedure to account for the differences that are found between the actual and initial scheduled reactive powers of motors. One solution [6] that has been put forward to solve the problem is to incorporate a steady-state model of induction motor in the initial power flow study in order to find the correct initial bus voltage in relation to the motor's actual reactive power. In this work, the Newton-Raphson algorithm has been used by taking into account the actual behavior of induction motors subject to a constant mechanical toque profile (motor's active power is assumed to remain unchanged with variation in the terminal voltage). Hence, in this method, the power flow solution is only limited with constant torque profile. In recent publication [7], a technique has been put forward to obtain the correct motor's reactive power in the PSS/E software package, which may also find application in other software packages that treat the induction motor as a PQ load. However, the method resorts to trial-and-error adjustments in the motor's reactive power and repetitive power flow calculations until a zero mismatch exists between the actual and initial reactive powers.

Hence, in this paper, the Newton-Raphon power flow algorithm has been further extended to incorporate the non-linear characteristics of the induction motor load. A variety of motor's mechanical torque profiles is accounted through the extended algorithm. The algorithm incorporates motor's slips, air-gap powers, and transient induced voltages that are automatically adjusted and updated during power flow iteration process. Moreover, the numerical result of 14buses industrial power system with a group of induction motors is demonstrated. The impacts of induction motor loads on the convergence characteristics of the extended power flow algorithm are investigated through the industrial power system and

Manuscript received on July 31, 2011 ; revised on November 11, 2011.

[1] The author is with the Department of electrical engineering, Thammasat University, Pathumthani, Thailand., E-mail: apichai@engr.tu.ac.th

IEEE-30buses test network.

2. INDUCTION MOTOR MODEL FOR POWER FLOW STUDY

The differential equation, describing motor nonlinear characteristic, can be given by [8],

equ1

$$\frac{d\tilde{E}'_m}{dt} = -\frac{1}{\tau'_m}\left(\tilde{E}'_m - j(X_{ss} - X')\tilde{I}_m\right) - js\omega_s\tilde{E}'_m \quad (1)$$

where,

$$\tilde{I}_m = \frac{\tilde{V}_m - \tilde{E}'_m}{R_s + jX'} \quad (2)$$

$$\tau'_m = \frac{X_{lr} + X_m}{\omega_s R_r} \quad (3)$$

$$X' = (X_{ss} - X_m^2)/(X_{lr} + X_m) \quad (4)$$

$$X_{ss} = X_{ls} + X_m \quad (5)$$

$$\tilde{V}_m = V_m e^{j\theta_m} \quad (6)$$

$$\tilde{E}'_m = E'_m e^{j\theta'_m} \quad (7)$$

Rearranging the motor's input current $\tilde{I}_m$ in term of steady-state condition by setting $d\tilde{E}'_m/dt = 0$ gives,

$$\tilde{I}_m = \left\{\frac{X_{lr} + X_m}{jX_m^2} + \frac{((X_{lr} + X_m)/X_m)^2}{R_r/s}\right\}\tilde{E}'_m \quad (8)$$

According to (2) and (8), the motor's equivalent circuit can be drawn as shown in Fig. 1. It consists of internal bus ($\tilde{E}'_m$), which represents transient induced voltage due to the motor current $\tilde{I}_m$. The motor's output is per-unit air-gap power P_{ag}. It is noted that the per-unit air-gap power is equal to the per-unit shaft torque since the synchronous speed is chosen as base quantity. In this paper, this equivalent circuit is used for the power flow calculation.

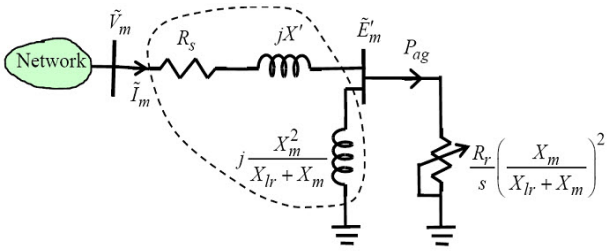

Fig.1: *Induction motor equivalent circuit*

3. NEWTON-RAPHSON ALGORITHM WITH INDUCTION MOTORS

This section demonstrates an extension of Newton-Raphson power flow algorithm to incorporate induction motors. Because motor's variables, such as the transient induced voltage ($\tilde{E}'_m$), phase angle (θ'_m), slip (s) are added, the nonlinear set [9] of function $\boldsymbol{f}(\mathbf{x})$can be written by,

$$\boldsymbol{f}(\mathbf{x}) = -\mathbf{J}(\mathbf{x})\boldsymbol{\Delta}\mathbf{x} \quad (9)$$

where,

$$\boldsymbol{f}(\mathbf{x}) = \begin{bmatrix} \mathbf{P}^{cal}_{l-n} - \mathbf{P}^{sche} \\ \mathbf{P}^{cal}_{l_m}(\mathbf{x}) - \mathbf{P}^{sche}_{mot}(\mathbf{x}) \\ \mathbf{Q}^{cal}_{l-n}(\mathbf{x}) - \mathbf{Q}^{sche} \\ \mathbf{Q}^{cal}_{l-m}(\mathbf{x}) - \mathbf{Q}^{sche}_{mot}(\mathbf{x}) \\ \mathbf{T}^{cal}_{mech}(\mathbf{x}) + \mathbf{T}^{sche}_{elec}(\mathbf{x}) \end{bmatrix} = \begin{bmatrix} \boldsymbol{\Delta}\mathbf{P} \\ \boldsymbol{\Delta}\mathbf{P_m} \\ \boldsymbol{\Delta}\mathbf{Q} \\ \boldsymbol{\Delta}\mathbf{Q_m} \\ \boldsymbol{\Delta}\mathbf{T_m} \end{bmatrix} \quad (10)$$

$$\mathbf{J}(\mathbf{x}) = [\{\mathbf{J}_{con}(\mathbf{x})\} + \{\mathbf{J}_{mot}(\mathbf{x})\}] \quad (11)$$

$$\boldsymbol{\Delta}\mathbf{x} = \begin{bmatrix} \boldsymbol{\Delta}\theta & \boldsymbol{\Delta}\theta'_{\boldsymbol{m}} & \boldsymbol{\Delta}\mathbf{V} & \boldsymbol{\Delta}\mathbf{E}'_{\boldsymbol{m}} & \boldsymbol{\Delta}\mathbf{s_m} \end{bmatrix}^T \quad (12)$$

The function $\boldsymbol{f}(\mathbf{x})$ in (9) gives the differences between the scheduled and the calculated quantities, known as mismatch. The superscripts *sche* and *cal* indicate scheduled and calculated, respectively. The subscripts 1-n and 1-m denote the total number of network buses and motor internal buses, respectively. The Newton-Raphson power flow algorithm can be modified as follows,

1. Incorporating motor's impedance enclosed by the dashed line in Fig. 1 into the network admittance matrix.
2. $P^{sche}_{mot}(\mathbf{x})$ is scheduled air-gap power (injected quantity) can be calculated by

$$P^{sche}_{mot}(x) = -\frac{((X_{lr} + X_m)/X_m)^2}{R_r/s}E'^2_m \quad (13)$$

   The scheduled reactive power $Q^{sche}_{mot}(x)$ of motor is zero since the element $jX_m^2/(X_{lr} + X_m)$ in Fig.1 is already integrated into the admittance matrix.
3. $T^{sche}_{elec}(\mathbf{x})$ and $T^{cal}_{elec}(\mathbf{x})$ are scheduled electrical torque and calculated mechanical torque of motors, which are given by,

$$T^{sche}_{elec}(\mathbf{x}) = -\frac{V_m E'_m}{R_s^2 + X'^2}\left\{\begin{pmatrix} R_s\cos(\theta_m - \theta'_m) + \\ X'\sin(\theta_m - \theta'_m) \end{pmatrix} - \begin{matrix} \\ R_s E'_m/V_m \end{matrix}\right\} \quad (14)$$

$$T^{cal}_{mech}(\mathbf{x}) = -T^0_m(A(1-s)^2 + B(1-s) + C) \quad (15)$$

The jacobain matrix $\mathbf{J}(\mathbf{x})$ consists of conventional jacobian matrix $\mathbf{J_{con}}(\mathbf{x})$ and motor-related jacobian matrix $\mathbf{J_{mot}}(\mathbf{x})$, which can be derived by differentiating the mismatches $\boldsymbol{\Delta}\mathbf{P_m}, \boldsymbol{\Delta}\mathbf{Q_m}$ and $\boldsymbol{\Delta}\mathbf{T_m}$ in (10).

4. POWER FLOW TEST CASE

In this section, the power flow solution obtained from the extended algorithm is demonstrated using 14buses industrial power system as illustrated in Fig. 2. The system parameters are given in Appendix A. The study system consists of slack bus (bus 1), PV bus (bus 2) and PQ bus (bus 3-14). The PQ buses are mainly connected with induction motor loads, whose parameters are also given in Appendix B.

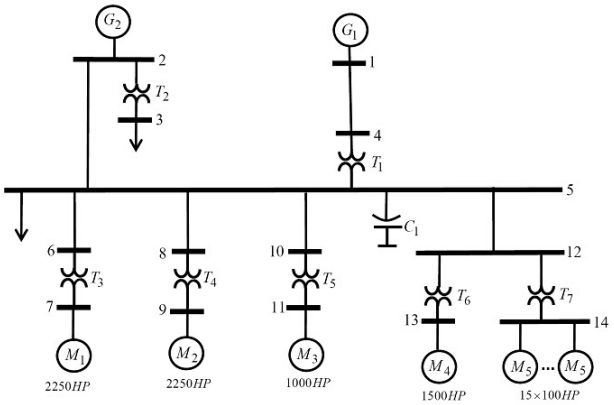

Fig.2: *14buses industrial power system*

In the power flow calculation, the internal induced voltage buses 15, 16, 17, 18, and 19 of induction motor loads in connection with buses 7, 9, 11, 13 and 14, respectively, are additionally created into the network. At first step, the initial values of motor's slips are computed by solving the steady-state torque equilibrium point using the rated voltage. The obtained slips are then employed, using the equivalent circuit in Fig. 1, to calculate the initial internal bus voltage of all motors for starting power flow calculation. For the rest of PQ buses, the normal flat voltage profiles (1.0pu.) are applied. In this study, the mechanical torque profiles of all motor loads are set as constant torque ($A = B = 0$ and $C = 1$) except those of motor M_2, whose torque profile is proportional to the square of speed ($A = 1$ and $B = C = 0$). After the power flow study successfully converges to a mismatch tolerance of $1.0E^{-10}$ in four iterations, the final solution is summarized in Table 1.

Table 1 shows voltage, angle, active (P) and reactive (Q) powers of all buses. The active and reactive powers of the first two buses (buses 1-2) are related to the generation but the rests are related to the demand of PQ buses. The transient internal induced voltage, phase angle, air-gap power, and slip of all motor loads are located at the buses 15-19. These quantities are automatically obtained after the power flow calculation is successfully converged. It is noted that active powers drawn from the motor's internal buses are known as air-gap powers. Since the equivalent circuits of all motor loads are directly embedded into the network admittance matrix, the reactive power demands drawn through the internal buses are zero, as seen from Table 1. The results obtained from the extended algorithm demonstrate the exact solution of the operating conditions of all different size motor loads in the industrial power system. The slips of all motors in the sixth column are exactly matched with their converged input voltages and air-gap powers since they are automatically adjusted during the power flow iteration. For example, although the electrical distance or impedances of feeder and transformer between bus 5 and motors M_1 and M_2 are equal, their obtained operating points, such as the internal bus voltages, slips, and air-gap powers, are distinct with regard to the different mechanical torque profiles being set. It can be seen that the motor M_1 with a constant torque profile has higher air-gap power (1.6785MW) than that (1.6524MW) of the motor M_2 with a square-of-speed torque profile. As expected, their input apparent powers are not equal. According to Table 1, the percent change of the motor's input MVA between M_1 and M_2 is founded by 1.5% due to the difference in their mechanical torque profiles. Moreover, Table 1 shows that, the air-gap powers of the individual large-size motor M_4 (1500HP) and the aggregated medium-size motor M_5 (15×100HP) are equal because both of them have the same equivalent horse power output and torque profile. However, the input reactive power of the aggregated M_5 (0.537MVAR) is higher than that of M_4 (0.447MVAR) by 20.1% since the motor M_5 operates with higher value of slip.

From the presented results, it can be said that the extended power flow algorithm gives the exact

Table 1: *Power Flow Solution of 14buses Power System*

Bus No.	volt pu.	angle deg.	P MW	Q MVAR	slip %
1	1.0000	0	6.6764	0.2107	-
2	0.9970	-2.1402	2.0	1.6835	-
3	0.9777	-3.3395	0.0	0.4	-
4	0.9990	-0.1117	2.0	0.0	-
5	0.9965	-2.1509	0.0	1.5	-
6	0.9962	-2.1556	0.0	0.0	-
7	0.9764	-4.3578	0.0	0.0	-
8	0.9963	-2.1555	0.0	0.0	-
9	0.9767	-4.3222	0.0	0.0	-
10	0.9964	-2.1522	0.0	0.0	-
11	0.9863	-3.0774	0.0	0.0	-
12	0.9963	-2.1544	0.0	0.0	-
13	0.9750	-4.3216	0.0	0.0	-
14	0.9718	-4.3055	0.0	0.0	-
15	0.9223	-13.327	1.6785	0.0	0.79
16	0.9231	-13.138	1.6524	0.0	0.78
17	0.9083	-13.637	0.373	0.0	1.53
18	0.9121	-14.399	0.119	0.0	0.91
19	0.9144	-10.865	1.119	0.0	5.42
From bus - To bus			Motor's input MVA $Se^{j\theta}$ or P+jQ		
7-15(M_1)			$1.8155e^{j20.77}$ or 1.697+j0.644		
9-16(M_2)			$1.7876e^{j20.82}$ or 1.671+j0.636		
11-17(M_3)			$0.4148e^{j23.04}$ or 0.382+j0.162		
13-18(M_4)			$1.2203e^{j21.48}$ or 1.136+j0.447		
14-19(M_5)			$1.2561e^{j25.33}$ or 1.135+j0.537		

amount of both active and reactive powers required by the individual induction motor loads. Thus, any artificial admittance added into the network admittance matrix is not necessary for adjusting the differences between the actual and scheduled powers, when initializing the power system dynamic studies including the induction motor loads.

To verify the computational accuracy of the power flow results given by the extended power flow algorithm, the converged solution of motor's active and reactive powers are used to re-calculate using the conventional algorithm, starting from the flat voltage profile. As expected, the power flow solutions obtained from both conventional and extended algorithms agree with each other, confirming the numerical accuracy of the computational results.

5. CONVERGENCE TEST

In this section, the computational performances between the conventional and extended Newton-Raphson algorithms are investigated and compared through their convergence characteristics. After the power flow solution is arrived using the extended algorithm, the converged motor's air-gap power together with active and reactive powers of all PQ buses are used as input quantities for recalculation, but in this times, using the conventional power flow algorithm. The absolute mismatches in (10) of 14buses industrial power system are plotted in Fig. 3 as a function of iteration numbers for the cases of the extended and conventional algorithms. Fig. 3 illustrates that the extended algorithm converges in quadratic manner as the conventional algorithm does. A slight difference in the mismatches is simply shown. Hence, the number of iteration is very close.

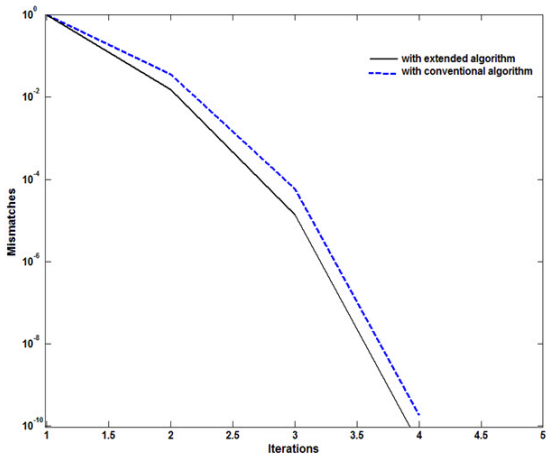

Fig.3: *Mismatches characteristic of 14buses system*

Next, the effects of induction motor loads on the convergence characteristic are further examined using the IEEE-30buses power network [10]. First, the most critical load bus, having the biggest influence on the power flow convergence, is identified using $Q-V$ sensitivity analysis in order to incorporate the motor motors. It is found that bus 30 is one of the most significant buses. Hence, the IEEE-30buses network is modified to incorporate the industrial subsystem (Fig. 2) into bus 30. The size of the network is now increased from 30 up to 49 buses (including motor's internal buses). The amount of active and reactive powers normally drawn by the constant power load at bus 30 is reallocated for the industrial system in such a way that the total amount remains the same (10.6MW and 2MVAR). The absolute mismatches of the unmodified and modified IEEE-30buses networks are plotted as shown in Fig. 4.

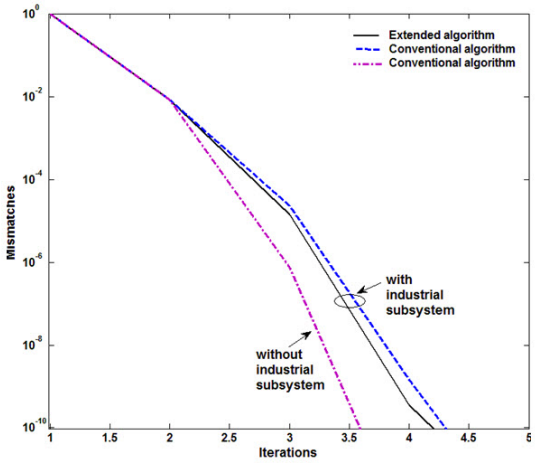

Fig.4: *Mismatches characteristic of unmodified and modified IEEE-30buses networks*

Firstly, let's consider the case where the IEEE-30buses network is not yet modified to incorporate the industrial subsystem. The mismatch (dashed-dotted line) in Fig. 4 reveals that the power flow calculation using the conventional Newton-Rapshon algorithm converges in 3 iterations at the given tolerance of 1.0E^{-10}. However, when the IEEE-30buses network is modified to include the industrial subsystem, the mismatches are all increased for the cases where the power flow solution is directly computed through the extended algorithm or re-simulated through the conventional algorithm. However, the convergence characteristic of the extended algorithm is satisfactory in quadratic manner. Moreover the mismatch of the extended algorithm is comparatively smaller than that of the conventional algorithm. Hence, it can be concluded that the extended algorithm does not only give correct active and reactive powers of induction motor loads but also preserve a convergent characteristic in quadratic manner.

6. CONCLUSION

The Newton-Raphson power flow algorithm has been extended to incorporate the nonlinear model of

the induction motors in this paper. The motor's slip, transient internal voltage, and a variety of torque profiles are embedded into the power flow jacobian matrix. The numerical results have been demonstrated using the 14buses industrial power system. The study results show that the extended algorithm gives correct motor's active and reactive powers that directly relate to motor's slip and internal bus voltage and torque profiles. Hence, it provides a proper way of initializing power system dynamic assessment. In additions, the extended algorithm shows a great capable of finding the steady-state operating conditions of a power system with a variety of motor mechanical torque profiles by a judicious selection of the torque coefficients. Furthermore, the studies are carried out using the IEEE-30buses system to demonstrate a computational efficiency. The extended algorithm exhibits quadratic convergence characteristics, in line with those of the conventional power flow algorithm.

7. ACKNOWLEDGEMENT

The work described in this paper was sponsored by Thammasat University academic affairs, 2011.

References

[1] C. W. Taylor, *Power system voltage stability*, McGraw-Hill, 1994.

[2] P. Kundur, *Power System Stability and Control*, McGraw-Hill, New York, 1993.

[3] IEEE Task Force on Load Representation for Dynamic Performance, "Load Representation for Dynamic Performance Analysis," *IEEE Trans. Power systems*, vol. 8, No. 2, pp. 472-482, 1993.

[4] IEEE Task Force on Load Representation for Dynamic Performance, "Standard Load Models for Power Flow and Dynamic Performance Simulation," *IEEE Trans. Power systems*, vol.10, No. 3, pp. 1302-1313, 1995.

[5] L. Pereira, D. Kosterev, P. Mackin, D. Davies, and J. Undrill, "An Interim Dynamic Induction Motor Model for Stability Studies in the WSCC," *IEEE Trans. Power Systems*, vol. 17, No. 2, pp.1108-1115, 2002.

[6] D. Ruiz-Vega, T. I. Asiain Olivares, and D. O. Salinas, "An Approach to the Initialization of Dynamic Induction Motor Models," *IEEE Trans. Power Systems*, Vol. 17, No. 3, pp. 747-750, 2002.

[7] J. Powell, and G. Radman, "Initialization for Dynamic Simulation of Stressed Power Systems Considering Induction Motor Components of Loads," *Power Symposium*, NAPS'07, 39th North American, pp. 102-107, 2007.

[8] J. Machowsky, J. W. Bialek, and J. R. Bumby, *Power System Dynamic and Stability*, John Wiley & Sons, 2008.

[9] A. R. Bergen, V. Vittal, *Power System Analysis*, Prentice Hall, New Jersey, 2000.

[10] Y. Wallach, *Calculation and Programs for Power System Networks*, Prentice-Hall, New York, 1986.

[11] G. J. Manno, and R. T.H. Alden, "An Aggregate Induction Motor Model for Industrial Plants," *IEEE Trans. Power Apparatus and systems*, Vol. 103, No. 4, pp.683-690, 1984.

APPENDIX A

Table A1: *Line cable (10MVA base)*

From	To	$R(pu)$	$X(pu)$
1	4	0.001390	0.00296
2	5	0.00122	0.00243
5	6	0.00118	0.00098
5	8	0.00118	0.00098
5	10	0.00157	0.00131
5	12	0.00075	0.00063

Table A2: *Transformer data*

Name	MVA	$Z(\%)$	X/R
T_1	15	8	17
T_2	1.5	5.75	6.5
T_3,T_4	2.5	5.75	10
T_5	1.5	6.75	6.5
T_6,T_7	1.725	6	8

Table A3: *Shunt capacitor (10MAV base)*

Name	G(pu)	B(pu)
C_1	0	0.3

Table A4: *Load*

Bus	MW	MVAR
3	0.6	0.4
5	2.0	1.5

Table A5: *Generation*

Bus	MW	V
2	2.0	0.997

APPENDIX B

Table B1: *Motor parameters (10MVA base)*

motor	R_s	$X_{ls} = X_{lr}$	X_m	R_r
M_1	0.0548	0.4276	24.6576	0.0416
M_2	0.0548	0.4276	24.6576	0.0416
M_3	0.4953	2.2805	102.1225	0.3535
M_4	0.1059	0.7126	37.5566	0.0699
M_5	0.0977	0.4751	22.4484	0.4222

Pichai Aree received his M.S.C. in electrical power engineering from the University of Manchester Institute Science and Technology (UMIST), England, in 1996, and P.h.D. degree in electrical engineering from the University of Glasgow, Scotland, in 2000. He joined Department of Electrical Engineering, Thammasat University (TU) in 1993. From June 2001 to May 2002, he was a visiting professor at the University of Alabama, at Birmingham, USA. He is currently an asociate professor at Department of Electrical Engineering, TU. His research interests are power system modeling, dynamics and stability.